



Far Field coherent thermal emission from a bilayer structure

Jérémie Drevillon, Karl Joulain, Philippe Ben-Abdallah, E. Nefzaoui

► To cite this version:

Jérémie Drevillon, Karl Joulain, Philippe Ben-Abdallah, E. Nefzaoui. Far Field coherent thermal emission from a bilayer structure. *Journal of Applied Physics*, 2011, 109 (3), pp.034315. 10.1063/1.3544359 . hal-00649364

HAL Id: hal-00649364

<https://hal-iogs.archives-ouvertes.fr/hal-00649364>

Submitted on 5 Apr 2012

HAL is a multi-disciplinary open access archive for the deposit and dissemination of scientific research documents, whether they are published or not. The documents may come from teaching and research institutions in France or abroad, or from public or private research centers.

L'archive ouverte pluridisciplinaire **HAL**, est destinée au dépôt et à la diffusion de documents scientifiques de niveau recherche, publiés ou non, émanant des établissements d'enseignement et de recherche français ou étrangers, des laboratoires publics ou privés.

Far field coherent thermal emission from a bilayer structure

J. Drevillon, K. Joulain, P. Ben-Abdallah, and E. Nefzaoui

Citation: *J. Appl. Phys.* **109**, 034315 (2011); doi: 10.1063/1.3544359

View online: <http://dx.doi.org/10.1063/1.3544359>

View Table of Contents: <http://jap.aip.org/resource/1/JAPIAU/v109/i3>

Published by the [American Institute of Physics](#).

Related Articles

Space charge and quantum effects on electron emission

J. Appl. Phys. **111**, 054917 (2012)

Enhanced electron field emission from plasma-nitrogenated carbon nanotips

J. Appl. Phys. **111**, 044317 (2012)

Field-emission properties of individual GaN nanowires grown by chemical vapor deposition

J. Appl. Phys. **111**, 044308 (2012)

High emission currents and low threshold fields in multi-wall carbon nanotube-polymer composites in the vertical configuration

J. Appl. Phys. **111**, 044307 (2012)

Experimental study on the field emission properties of metal oxide nanoparticle-decorated graphene

J. Appl. Phys. **111**, 034311 (2012)

Additional information on J. Appl. Phys.

Journal Homepage: <http://jap.aip.org/>

Journal Information: http://jap.aip.org/about/about_the_journal

Top downloads: http://jap.aip.org/features/most_downloaded

Information for Authors: <http://jap.aip.org/authors>

ADVERTISEMENT



**FIND THE NEEDLE IN THE
HIRING HAYSTACK**

Post jobs and reach
thousands of hard-to-find
scientists with specific skills



<http://careers.physicstoday.org/post.cfm> **physicstoday JOBS**

Far field coherent thermal emission from a bilayer structure

J. Drevillon,^{1,a)} K. Joulain,¹ P. Ben-Abdallah,² and E. Nefzaoui¹¹Département Fluides, Thermique, Combustion, Institut Pprime, CNRS–Université de Poitiers–ENSMA, ENSIP-Bâtiment B25, 2, rue Pierre Brousse, F 86022 Poitiers Cedex, France²Laboratoire Charles Fabry, Institut d'Optique, CNRS, Université Paris-Sud, Campus Polytechnique, RD128, F 91127 Palaiseau Cedex, France

(Received 24 June 2010; accepted 11 December 2010; published online 11 February 2011)

Recent years, there has been an increased interest in the conception of micro/nanostructures with unusual radiative properties, far away from those of blackbody, especially thermal sources with temporal and/or spatial coherent emission. Such structures are indeed extremely interesting for energy conversion systems, radiative cooling devices, etc. The present study numerically investigates temporal coherent emission from a very simple structure composed of one layer of germanium and one of silicon carbide. Our investigation shows that, for well-defined thicknesses, this two-layer structure is able to emit in narrow spectral peak. © 2011 American Institute of Physics. [doi:10.1063/1.3544359]

I. INTRODUCTION

Enhancement of thermal emission and/or control of its direction is undoubtedly one of the major objectives in improving the efficiency of numerous nowadays technologies such as thermophotovoltaic conversion devices, radiative cooling systems, and radiation detectors. Until recently, thermal sources were considered as objects that were able to emit light only over a broad band of the infrared spectrum. Today we know this paradigm is wrong^{1,2} and several partially coherent thermal sources have been already fabricated.^{3–5} The origin of these unusual behaviors comes from the micro or nanostructuring of the materials used to fabricate these sources.^{6–8} Coherent emission is associated with sharp spectral peaks (temporal coherence) and/or narrow angular lobes in well-defined directions (spatial coherence). Coherent thermal emission has been demonstrated using gratings,^{4,9,10} by excitation and diffraction in the far field of surface polaritons. However these effects are based on optical mechanisms which strongly limit their applications in the field of thermal emission.

Left-handed material¹¹ which are engineered from one-dimensional (1D) periodic metallic structures and which have a refractive index much less than unit have also been developed as coherent thermal sources but experimental demonstration was only realized in the microwave domain. Recently, negative-index metamaterials have been achieved in the near-infrared region¹² and with the recent advances in the metamaterials conception, theoretical studies to tailor the thermal emission based on metamaterials were realized.¹³

The use of photonic crystals¹⁴ (PCs) has allowed to make a breakthrough in the design of coherent thermal sources. At sufficient refractive index contrast, PCs forbid photons to propagate through them at certain wavelengths, irrespective to propagation direction in space and polarization. Coupled with frequency selective surfaces, PCs have recently allowed the construction of narrow bands IR

emitters.¹⁵ These past years' promising results have opened prospects for the fabrication of temporally coherent infrared sources where a structural defect is introduced into a PC.^{16–18} Such defects act like waveguides with a confinement achieved by means of the photonic band gap and not by total internal reflection as in traditional waveguides. It was also demonstrated recently that a polar material coupled with a semi-infinite PC could act as a partially coherent thermal source.^{19,20} These structures exhibit highly directional and narrow band emission patterns for both TM and TE polarization states of the thermal light. Similar antennalike emission patterns also have been achieved with completely different physical mechanisms using simple thin films²¹ and more recently resonant cavities coupled with metallic layers.²² The coupling of a surface grating with a waveguide also permits, theoretically, to obtain a temporal and spatial coherent thermal source.²³ More recently a general method for the *ab initio* design of coherent thermal sources by using only the first principles of optics was developed.²⁴ Numerical experiments, based on a genetic algorithm, demonstrated that it is possible to predict the inner structure of nanolayered thermal sources in order to control both emission, reflection, and transmission properties. However, thermal sources designed until now has an internal structure that remains rather complex for a large scale production, considering existing nanofabrication techniques.

II. THE BILAYER STRUCTURE

The present study investigates spectral coherent emission in midinfrared of a 1D structure composed of two layers only (Fig. 1). The first layer is made of germanium (Ge) and the second layer is made of silicon carbide (SiC). In the infrared wavelength range under investigation ($[8\ \mu\text{m}, 14.5\ \mu\text{m}]$), Ge is a nonemitting (transparent) material and its dielectric permittivity can be approximated²⁵ by a constant value $\epsilon_{\text{Ge}}=16$. As for the SiC, it is the only dissipative material and its dielectric function is correctly described by the simple oscillating Lorentz model as follows:²⁵ $\epsilon(\omega)=\epsilon_{\infty}[1$

^{a)}Electronic mail: jeremie.drevillon@univ-poitiers.fr.

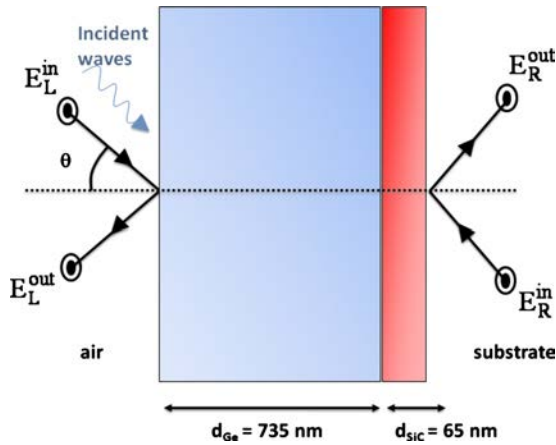


FIG. 1. (Color online) Quasimonochromatic thermal source made with germanium (thickness of 735 nm) and silicon carbide (thickness of 65 nm). In the region of infrared spectrum under investigation Germanium is a non-emitting (transparent) material ($\epsilon_{\text{Ge}}=16$). As for the SiC, it is the only dissipative material and its dielectric function is correctly described by the simple oscillating Lorentz model.

$+\omega_L^2 - \omega_T^2 / \omega_T^2 - \omega^2 - i\Gamma\omega]$, where $\omega_L = 18.253 \times 10^{13} \text{ rad s}^{-1}$, $\omega_T = 14.937 \times 10^{13} \text{ rad s}^{-1}$, $\Gamma = 89.66 \times 10^{10} \text{ rad s}^{-1}$, and $\epsilon_\infty = 6.7$, denote the longitudinal and transversal optical phonon pulsation, the damping factor, and the high frequency dielectric constant, respectively. All materials involved here are nonmagnetic in this wavelength range.

We remind hereafter the basic principles for the calculation of the spectral and directional emissivity $\epsilon(\lambda, \theta)$, reflectivity $\rho(\lambda, \theta)$, and transmittivity $t(\lambda, \theta)$ of this structure. These radiative properties are calculated from the transfer matrix $\mathcal{J}(0, L)$ of the whole structure for both polarization states. True optical signature of the structure, the matrix $\mathcal{J}(0, L)$ connects incoming electric field $\mathbf{E}_L(E_L^{\text{in}}, E_L^{\text{out}})$ on the left-hand side of the structure to emerging field $\mathbf{E}_R(E_R^{\text{in}}, E_R^{\text{out}})$ on its right-hand side by a relation of the form

$$\begin{pmatrix} E_L^{\text{in}} \\ E_L^{\text{out}} \end{pmatrix} = \mathcal{J}(0, L) \begin{pmatrix} E_R^{\text{in}} \\ E_R^{\text{out}} \end{pmatrix}. \quad (1)$$

This matrix relation is perfectly well adapted to the composition of elementary networks corresponding to a piling up process. Thus, the transfer matrix of the whole structure is the result of product $\mathcal{J}(0, L) = \prod_{i=1}^5 \mathcal{J}_{\text{sub}}(i)$ of elementary transfer matrix $\mathcal{J}_{\text{sub}}(i)$, which describes either the crossing of an interface between two media

$$\mathcal{J}_{\text{cross}} = \frac{1}{t_{ij}} \begin{pmatrix} 1 & r_{ij} \\ t_{ij} & 1 \end{pmatrix} \quad (2)$$

or the phase shift in field across a layer

$$\mathcal{J}_{\text{prog}} = \begin{pmatrix} e^{i\phi_j} & 0 \\ 0 & e^{-i\phi_j} \end{pmatrix}. \quad (3)$$

Here, t_{ij} and r_{ij} are the transmission and reflection Fresnel coefficients,²⁶ respectively, at the interface between the medium i and the medium j and ϕ_j stands for the phase shift in waves across the layer j . It follows that the spectral and directional transmittivity $t(\lambda, \theta)$ and reflectivity $\rho(\lambda, \theta)$ of a structure are given in terms of transfer matrix compo-

nents by $t = |(E_R^{\text{out}})/(E_L^{\text{in}})|^2 = |1/(\mathcal{J}_{11})|^2$ and $\rho = |(E_L^{\text{out}})/(E_L^{\text{in}})|^2 = |(\mathcal{J}_{21})/(\mathcal{J}_{11})|^2$. Moreover, from Kirchhoff's law, we know that the directional and spectral emissivity $\epsilon(\lambda, \theta)$ is given by $\epsilon = \alpha = 1 - \rho - t$, where α denotes the absorptivity of the structure.

For our bilayer structure, \mathcal{J}_{11} can be expressed as follows

$$\mathcal{J}_{11} = \frac{e^{i(\gamma_2 d_2 + \gamma_3 d_3)}}{t_{12} t_{23} t_{34}} [1 - r_{21} r_{23} e^{-2i\gamma_2 d_2} - r_{32} r_{34} e^{-2i\gamma_3 d_3} - r_{21} r_{34} e^{-2i(\gamma_2 d_2 + \gamma_3 d_3)}]. \quad (4)$$

III. RESULTS

In Fig. 2, we present the spectral and directional emissivity and reflectivity for both polarizations of this bilayer structure. We can observe a very sharp emissivity peak centered around $\lambda^* = 12.61 \mu\text{m}$, the wavelength of upper edge of the phonons absorption band in SiC and with a maximum of emissivity $\epsilon_{\text{max}} = 0.95$. As for the reflexion spectrum we remark the presence, on both sides of λ^* , of large and quasicomplete (omnidirectional) photonic band gaps (except at oblique incidences), one between $[12.7 \mu\text{m}, 14.5 \mu\text{m}]$ and the other between $[8 \mu\text{m}, 12.5 \mu\text{m}]$. So far, such omnidirectional photonic band gaps had been observed only for rather complex structures such as multilayered media identified by inverse design,²⁴ in periodic materials,¹⁴ PCs with defect,²¹ and quasicrystals.²⁷⁻²⁹ This band gap is clearly desirable in the perspective of using this nanostructure as coating material.

Consequently, we succeed in the design of a quasi-isotropic temporal coherent thermal source composed simply of two layers and thus easier to fabricate with techniques of thin film deposition. We now take a look at the emission spectrum sensitivity to the thickness of the two layers. In Fig. 3 is presented the emissivity at normal incidence ($\theta = 0^\circ$) versus the Ge layer thickness. It may be noted that the amplitude of the emission peak strongly depends on the germanium thickness, with a maximum (at $\lambda^* = 12.61 \mu\text{m}$) for $d_{\text{Ge}} \approx 735 \text{ nm}$. The amplitude remains above 0.8 for thicknesses between 640 and 840 nm. Thus, we can tolerate a Ge thickness variation of 200 nm around the optimum without the spectral coherence of the thermal emission being questioned. This tolerance for Ge thickness on the emissivity properties will thus allow a margin error in the fabrication process of the structure. We also observe that emittance and reflectance oscillate (in opposite phase) and that others peaks appear for $d_{\text{Ge}} \approx (2N+1) \times 735 \text{ nm}$, $N=0, 1, 2, \dots$. Consequently, it will be possible to conceive coherent thermal bilayer sources with greater thicknesses if necessary.

These observations under normal incidence are also valid for the other incidence angles. Indeed, due to refraction laws, the incident rays penetrate the structure with a maximum angle $\theta_{\text{max}} = \arcsin(1/n_{\text{Ge}}) = 14^\circ$. Consequently, the photons interact with the SiC layer near normal incidence.

Let us now look at the influence of SiC thickness. We can observe in Fig. 4(a) that, at normal incidence, it has little influence on the emissivity amplitude, except for low thicknesses ($d_{\text{SiC}} < 200 \text{ nm}$). We can also observe in the Fig. 4, particularly for low thicknesses, that the highest emissivity

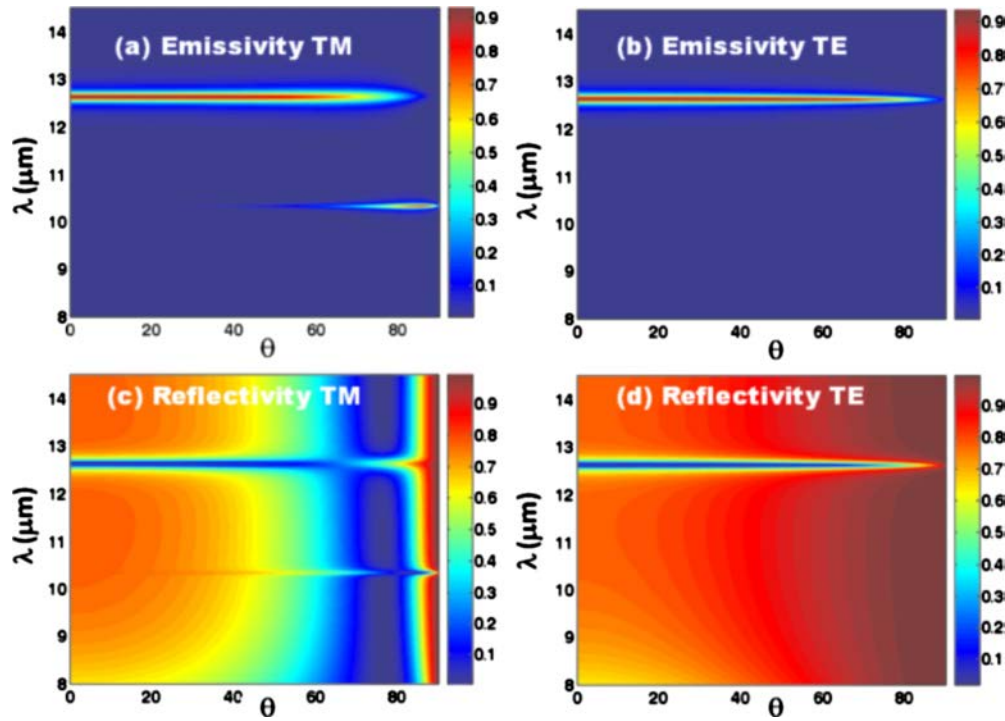


FIG. 2. (Color online) Spectral and directional emissivity for (a) TM and (b) TE polarization, and reflectivity for (c) TM and (d) TE polarization of a quasimonochromatic thermal source made of one layer of germanium and one layer of silicon carbide.

resonance according to SiC thickness depends on the wavelength. For example, at $\lambda^*=12.61 \mu\text{m}$, $d_{\text{SiC}}=65 \text{ nm}$ is the best SiC thickness but at $\lambda^*=12.63 \mu\text{m}$, the maximum amplitude of emissivity is reached for thicknesses greater than 250 nm. Indeed, if we look at the Fig. 4(b) we can see that the emission peak shifts slightly according to d_{SiC} . Furthermore, the emission spectrum coherence decreases when the SiC thickness increases, particularly for d_{SiC} greater than 200 nm. Finally, as shown in Fig. 5, increasing the size of the SiC layer causes a loss of coherence whatever the angle of emission. That is why we have chosen $d_{\text{Ge}}=735 \text{ nm}$ and $d_{\text{SiC}}=65 \text{ nm}$ as best achievable bilayer structure, but it is impor-

tant to note that until $d_{\text{SiC}}=200 \text{ nm}$, the bilayer structure remains a very good coherent thermal source.

IV. ANALYSIS

The coherent emission of the bilayer structure and the large dependence with the Germanium thickness appears to be due to antireflection effect^{26,30} and can recall the Salisbury screen properties,^{31,32} even if the underlying physics is not the same. Indeed, if we consider the simple case of a coating on a substrate immersed in air and assume radiation is incident at normal incidence, the reflectivity is given by the following:

$$R'_\lambda = \left| \frac{r_{12} + r_{23}e^{-2i\gamma_2 d}}{1 - r_{21}r_{23}e^{-2i\gamma_2 d}} \right|^2, \quad (5)$$

where $r_{ij}=(n_i-n_j)/(n_i+n_j)$ are the Fresnel reflexion coefficients for normal incidence, d the coating thickness and γ_2 the wave vector normal component in medium 2. Plotting the variation in R'_λ versus d , we can observe that reflectivity oscillates with the coating thickness with a period $\Delta d = \lambda/(2 \times n_2)$. If $n_1 < n_2 < n_3$, the reflectivity reaches a minimum at $d = \lambda(2N+1)/(4 \times n_2)$, $N=0,1,2,\dots$. Furthermore, if $n_2 = \sqrt{n_1 n_3}$, the reflectivity minimum becomes zero.

Taking $n_1=n_{\text{air}}=1$, $n_2=n_{\text{Ge}}=4$ and considering $n_3 \approx n'_{\text{SiC}}$, the real part of SiC refractive index (at $\lambda=12.61 \mu\text{m}$, $n'_{\text{SiC}} \approx 16$), the two conditions $n_{\text{air}} < n_{\text{Ge}} < n'_{\text{SiC}}$ and $n_{\text{Ge}} = \sqrt{n_{\text{air}} n'_{\text{SiC}}}$ are respected. In the simple case of a Ge slab on a substrate, the first optimal thickness for which we have a minimum reflectivity is $d_{\text{Ge}} = \lambda/(4 \times n_{\text{Ge}}) = 790 \text{ nm}$. However this optimal thickness is valid when we consider no absorption for SiC and a semi-infinite material. Due to the absorption of SiC in our case, the optimal thickness shifts

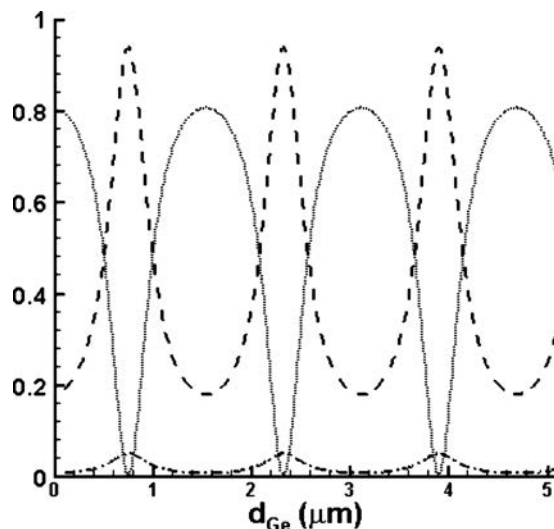


FIG. 3. Emissivity (dashed), reflectivity (dotted), and transmittivity (dashed-dotted) of the bilayer structure at the wavelength $\lambda^*=12.61 \mu\text{m}$ and under normal incidence ($\theta=0^\circ$) vs the thickness of germanium layer.

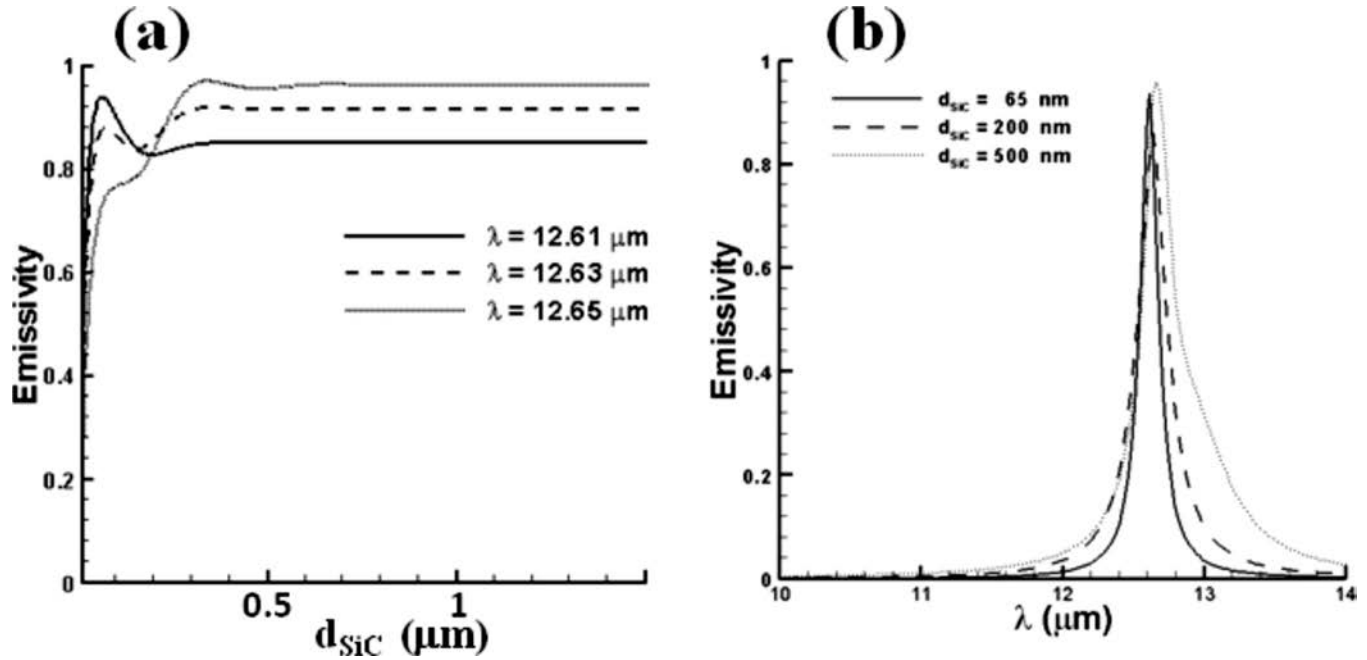


FIG. 4. Emissivity of the bilayer structure under normal incidence vs the thickness of silicon carbide layer (a) and vs the wavelength (b).

slightly and we observe a minimum reflectivity (and so a maximum emissivity) for $d_{\text{Ge}} = 735 \text{ nm}$. The SiC thickness influence on the emissivity resonance is weaker than that of germanium. To understand this different behavior, we must look at the penetration depth of electromagnetic waves in the material. The penetration depth is $\delta_\lambda = \lambda / (2\pi n''_{\text{SiC}})$ (n''_{SiC} is the imaginary part of refractive index). For wavelengths between 12.6 and $12.64 \mu\text{m}$, absorption is very important and n''_{SiC} varies greatly. Therefore δ_λ varies between 50 and 200 nm . That is why, for SiC layers greater than 200 nm , the

thickness does not affect much the results. On the other hand, for d_{SiC} order of δ_λ , the emissivity resonance can be slightly modified, but the peak amplitude remains very high anyway. It is also important to note that, as seen in Fig. 6, the SiC absorption decreases extremely rapidly and consequently the penetration depth increase also rapidly (at $\lambda = 12.61 \mu\text{m}$, $n''_{\text{SiC}} = 16$, and $\delta_\lambda = 125 \text{ nm}$ whereas at $\lambda = 13 \mu\text{m}$, $n''_{\text{SiC}} = 0.36$ and $\delta_\lambda = 5.7 \mu\text{m}$). Thus, when d_{SiC} increases, the number of resonant modes increases like in a Fabry–Perot resonator. Each of these guide modes participate to the bi-

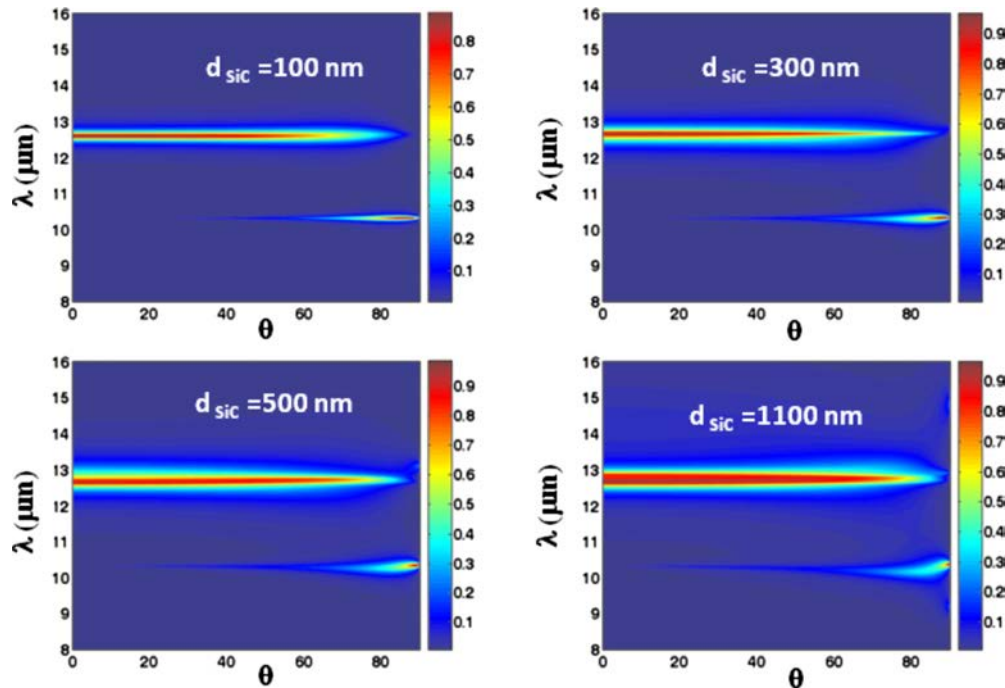


FIG. 5. (Color online) Spectral and directional emissivity in polarization TM of the bilayer structure made with one layer of germanium and one layer of silicon carbide with four different thickness d_{SiC} .

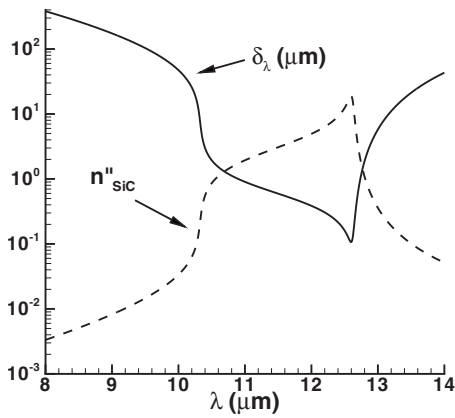


FIG. 6. Penetration depth (solid line) in SiC layer and SiC refractive index imaginary part (dashed line) vs the wavelength.

layer emission. The SiC film also behaves as a waveguide. Higher thicknesses allow more modes to propagate and leads to a coherence loss. To corroborate this interpretation, we have calculated the dispersion relations of propagative resonant modes of the whole structure and we can effectively see in Fig. 7 that the number of these modes increases with the SiC thickness like in a Fabry–Perot resonator.

This interpretation is finally confirmed by the magnitude of the inner electric field under external unit excitation. The electric field distribution within the structure when it is

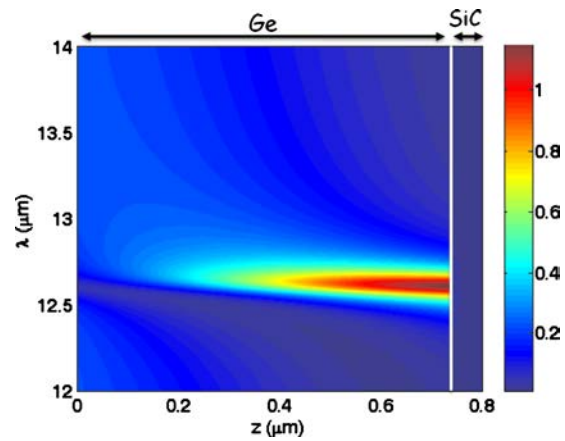


FIG. 8. (Color online) Modulus of the electric field polarization inside the bilayer structure (Ge/SiC) when it is highlighted by an incoming field of unit magnitude and under an angle of 0° .

lighted up by an incoming field of unit amplitude is calculated using the reflectivity coefficient r of the whole structure and the partial transfer matrix $\mathcal{T}(0, z)$ from the highlighted side at $z=0$ and the current point. The local electric field is then given by

$$E(z, \lambda, \theta) = \frac{\mathcal{T}_{22} + \mathcal{T}_{21} - r(\lambda, \theta)(\mathcal{T}_{11} + \mathcal{T}_{12})}{\det[\mathcal{T}]} \quad (6)$$

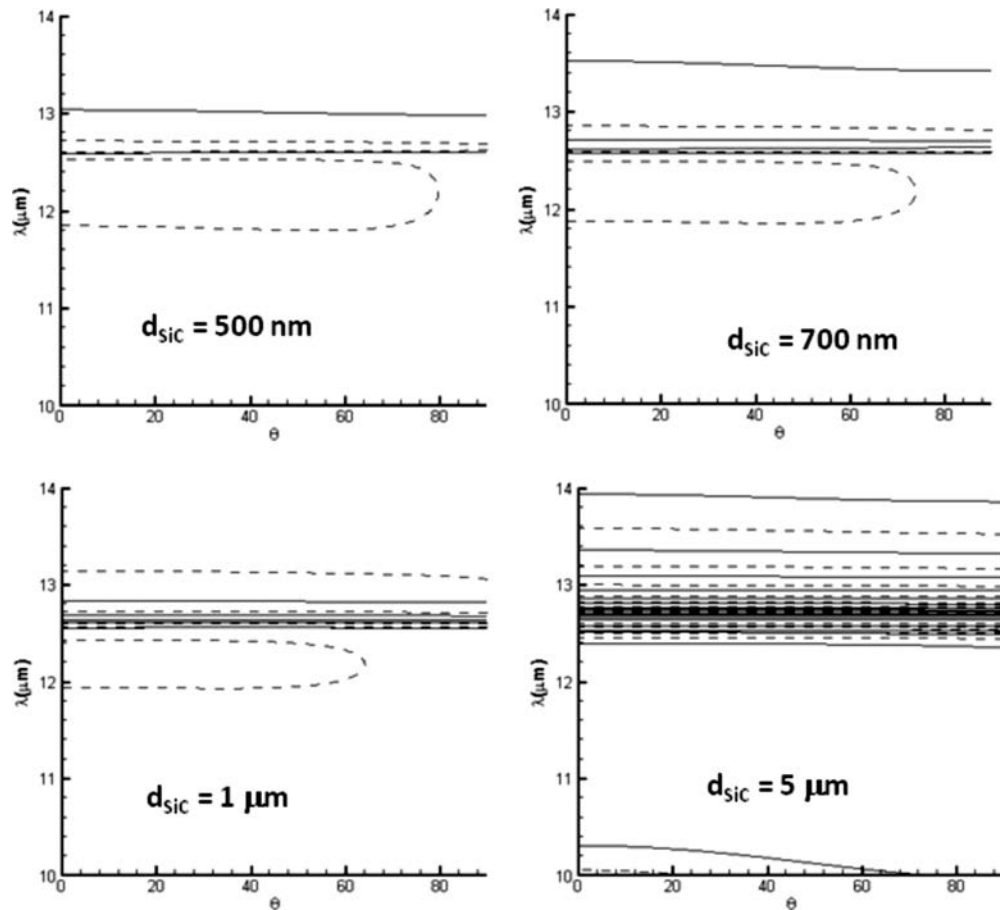


FIG. 7. Dispersion relations of propagative resonant modes in TE polarization with $d_{\text{Ge}}=735$ nm. In dotted line is plotted the real part of the equation $\mathcal{T}_{11}=0$ while in solid line is represented its imaginary part.

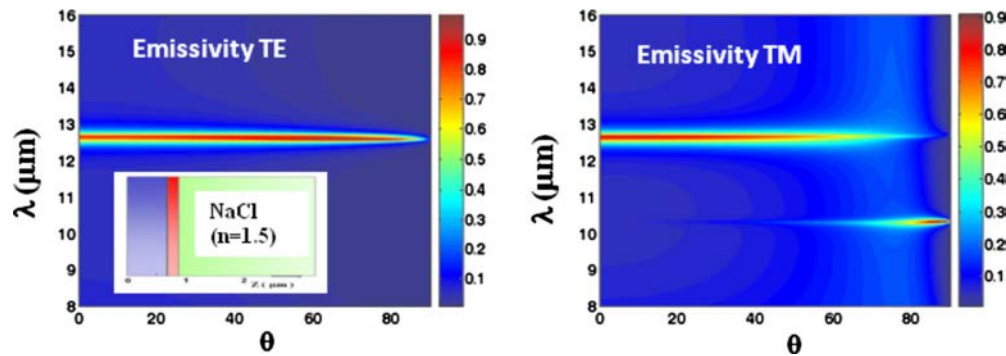


FIG. 9. (Color online) Spectral and directional emissivity of the bilayer structure (Ge/SiC) on a NaCl substrate. NaCl is transparent (real refractive index $n=1.5$) in the range of wavelength considered.

The result displayed in Fig. 8 shows that the intensity of the electric field inside the structure becomes locally much larger than one at the incidence angles and wavelengths where the emissivity spectrum is maximum. As we can see in this figure, this is due to internal resonances. Indeed, if we pay attention to the case where an incident wave of wavelength $\lambda^*=12.61 \mu\text{m}$ impinges the structure under an angle of 0° , we observe that the field amplitude at the interface between the SiC and Ge layers at $z=0.735 \mu\text{m}$ is enhanced. Such a resonance, localized on the interface Ge/SiC, reveals the presence of modes that are able to couple with the incident wave. Thus, the energy of this propagative wave is absorbed by the SiC layer. Therefore, this coupling directly contributes to the strong emission of the structure at λ^* . In contrast, for all other wavelengths in the domain $[8 \mu\text{m}, 14.5 \mu\text{m}]$, there is no significant enhancement of the electric field in the structure and very few energy is absorbed by the SiC layer. Consequently, according to Kirchhoff's law, the thermal emission of the structure is very small.

V. INFLUENCE OF A SUBSTRATE

In order to be able to achieve this thermal source in the near future, we are also interested in the possible impact on the peak emissivity observed numerically when this structure is deposited on a substrate. Therefore, we calculate the radiative properties of the bilayer structure located in the vacuum on the side of germanium and on the other side, on a substrate of sodium chloride (NaCl) (Fig. 9 inset). This material is transparent (real refractive index $n_{\text{NaCl}}=1.5$) in the range of wavelength under investigation. The thickness of the substrate is considered very large compared to the size of the structure and was modeled as a semi-infinite media. We may then observe (Fig. 9) the directional spectral emissivity of the bilayer structure (for both TE and TM polarization) has changed a little but the emission peak is always extremely narrow with a very high amplitude. However it is important to note that for substrates with greater refractive index, the radiative properties of the bilayer seem to deteriorate pointedly. A substrate with a relatively low dielectric permittivity is therefore preferred to maintain the temporal coherence of this quasimonochromatic thermal source.

VI. CONCLUSION

We have shown numerically that it is possible to design an extremely spectrally coherent thermal source by choosing wisely to stack two different materials, one emitting in the wavelength range under investigation, the other lossless in that range. This very simple internal structure could be extremely attractive in terms of manufacture with techniques for thin film deposition. It was further revealed that the thickness influence on the narrow peak of emission was sufficiently low to satisfy the constraints of nanofabrication techniques. The prospects to this work are, as a first step, the design of the coherent thermal source presented here to corroborate the numerical results but also the development of other coherent thermal “bilayer” sources emitting in other frequency domains. To do this, a new inverse design tool is under development and should enable the conception of several coherent thermal sources with extremely simple inner structuration.

- ¹R. Carminati and J. J. Greffet, *Phys. Rev. Lett.* **82**, 1660 (1999).
- ²A. V. Shchegrov, K. Joulain, R. Carminati, and J. J. Greffet, *Phys. Rev. Lett.* **85**, 1548 (2000).
- ³H. Sai, H. Yugami, Y. Akiyama, Y. Kanamori, and K. Hane, *J. Opt. Soc. Am. A* **18**, 1471 (2001).
- ⁴J. J. Greffet, R. Carminati, K. Joulain, J. P. Mulet, S. Mainguy, and Y. Chen, *Nature (London)* **416**, 61 (2002).
- ⁵K. Richter, G. Chen, and C. L. Tien, *Opt. Eng. (Bellingham)* **32**, 1897 (1993).
- ⁶P. Hesketh, J. Zemel, and B. Gebhart, *Nature (London)* **324**, 549 (1986).
- ⁷K. T. R. O. Buckius, *Nanoscale Microscale Thermophys. Eng.* **2**, 245 (1998).
- ⁸R. Dimenna and R. Buckius, *J. Heat Transfer* **116**, 639 (1994).
- ⁹J. Le Gall, M. Olivier, and J.-J. Greffet, *Phys. Rev. B* **55**, 10105 (1997).
- ¹⁰M. Kreiter, J. Oster, R. Sambles, S. Herminghaus, S. Mittler-Neher, and W. Knoll, *Opt. Commun.* **168**, 117 (1999).
- ¹¹S. Enoch, G. Tayeb, P. Sabouroux, N. Guérin, and P. Vincent, *Phys. Rev. Lett.* **89**, 213902 (2002).
- ¹²S. Zhang, W. Fan, N. C. Panoiu, K. J. Malloy, R. M. Osgood, and S. R. J. Brueck, *Phys. Rev. Lett.* **95**, 137404 (2005).
- ¹³B. Lee, L. Wang, and Z. Zhang, *Opt. Express* **16**, 11328 (2008).
- ¹⁴S. John, *Phys. Rev. Lett.* **58**, 2486 (1987); E. Yablonovitch, *ibid.* **58**, 2059 (1987); H. Benisty, S. Kawakami, D. Norris, and C. Soukoulis, *Photonics Nanostruct. Fundam. Appl.* **2**, 57 (2004).
- ¹⁵M. U. Pralle, N. Moelders, M. P. McNeal, I. Puscasu, A. C. Greenwald, J. T. Daly, E. A. Johnson, T. F. George, D. Choi, I. El-Kady, and R. Biswas, *Appl. Phys. Lett.* **81**, 4685 (2002).
- ¹⁶L. McCall, P. M. Plazman, R. Dalichaouch, D. Smith, and S. Schultz, *Phys. Rev. Lett.* **67**, 2017 (1991).
- ¹⁷E. Yablonovitch, T. J. Gmitter, R. D. Meade, K. D. B. A. M. Rappe, and J. D. Joannopoulos, *Phys. Rev. Lett.* **67**, 3380 (1991).

- ¹⁸P. Ben-Abdallah and B. Ni, *J. Appl. Phys.* **97**, 104910 (2005).
- ¹⁹B. J. Lee, C. J. Fu, and Z. M. Zhang, *Appl. Phys. Lett.* **87**, 071904 (2005).
- ²⁰C. J. Fu, Z. M. Zhang, and D. B. Tanner, *Opt. Lett.* **30**, 1873 (2005).
- ²¹P. Ben-Abdallah, *J. Opt. Soc. Am. A* **21**, 1368 (2004).
- ²²I. Celanovic, D. Perreault, and J. Kassakian, *Phys. Rev. B* **72**, 075127 (2005).
- ²³K. Joulain and A. Loizeau, *J. Quant. Spectrosc. Radiat. Transf.* **104**, 208 (2007).
- ²⁴J. Drevillon and P. Ben-Abdallah, *J. Appl. Phys.* **102**, 114305 (2007).
- ²⁵E. D. Palik, *Handbook of Optical Constants of Solids* (Academic, London, 1998).
- ²⁶P. Yeh, *Optical Waves in Layered Media* (Wiley-Interscience, New York, 1988).
- ²⁷W. Gellermann, M. Kohmoto, B. Sutherland, and P. C. Taylor, *Phys. Rev. Lett.* **72**, 633 (1994).
- ²⁸T. Hattori, N. Tsurumachi, S. Kawato, and H. Nakatsuka, *Phys. Rev. B* **50**, 4220 (1994).
- ²⁹A. Della Villa, S. Enoch, G. Tayeb, V. Pierro, V. Galdi, and F. Capolino, *Phys. Rev. Lett.* **94**, 183903 (2005).
- ³⁰Z. M. Zhang, *Nano/Microscale Heat Transfer* (McGraw-Hill, New York, 2007).
- ³¹A. Bauer, *Am. J. Phys.* **60**, 257 (1992).
- ³²M. Laroche, Role des ondes de surface dans la modification des propriétés radiatives de matériaux microstructures. Application à la conception de sources infrarouges et à l'effet thermophotovoltaïque, Ph.D. thesis, Ecole Centrale Paris, 2005.